

Calculation and analysis of microphysical and optical characteristics of atmospheric aerosol: the model of homogeneous spherical particles

S.A. Beresnev, L.B. Kochneva, and P.E. Suetin

Ural State University, Ekaterinburg

Received November 27, 2001

The calculations of microphysical and optical characteristics performed based on Lorenz–Mie theory (the internal field intensity, the absorption efficiency factor, the photophoretic asymmetry factor, and the light pressure factor) for some reference types of atmospheric aerosol are presented. To simplify the analysis, a model of homogeneous spherical particles is used. The analysis performed allows one to establish general regularities in the behavior of the above-mentioned characteristics for strongly, moderately, and weakly absorbing particles. Special attention is given to analysis of the photophoretic asymmetry factor J_1 . The features in J_1 behavior for reference types of the atmospheric aerosol are detected. In particular, for particles with $n = 1.5$ – 3.0 and $\kappa = 0.01$ – 0.1 the possibility of both negative ($J_1 > 0$) and positive ($J_1 < 0$) photophoresis is considered. The results obtained are planned to be used in the development of a model of vertical transport of the stratospheric aerosol.

Introduction

Minimum necessary complex of parameters can be selected among the microphysical and optical characteristics (MOC) responsible to the dynamics of particles in the field of directed electromagnetic radiation.¹ They are the following: source function of the electromagnetic energy in the particle volume $B(\mathbf{r})$ (or the intensity of internal field $I(r)$), radiation absorption efficiency factor Q_{abs} , light pressure efficiency factor Q_{pr} , and the asymmetry factor of the radiation absorption J_1 responsible for the photophoretic motion of particles. All of them, including partially the factor Q_{pr} are related to radiation not scattered but absorbed by a particle. Let us note that the necessity of analysis of the complex but not selected optical characteristics of particles was noted earlier.^{2,3} Such an approach allows us to reveal general regularities of the dependences of the characteristics on the determining parameters for particles of different types.

Such characteristics as $B(\mathbf{r})$ and Q_{abs} are quite well studied not only for optically homogeneous but also for multi-layer spherical particles (for example, Refs. 4 and 5), but no systematic study of the J_1 factor was carried out up to date. In this connection, it seems justified to use the models of optically homogeneous spherical particles in calculating full complex of MOC. Then, the possibility appears of analyzing the absorbing properties (and their consequences) of the particles of the principal types of atmospheric aerosol from the unified standpoints, which is the purpose of this paper.

Methods and algorithms for calculating the microphysical optical characteristics

The parameters $I(r)$, Q_{abs} , Q_{pr} , and J_1 were calculated depending on the values of the diffraction parameter $\rho = 2\pi R_0/\lambda$ by means of the Lorenz–Mie

theory⁶ for the particles of different types of atmospheric aerosol with reliably known values of the complex refractive index $m(\lambda) = n + ik$ at the wavelength of the incident radiation from 0.5 and 10.6 μm . A number of tested and effective algorithms^{6,7} are known for calculation of these MOC. These are capable of calculating the characteristics related to both absorbed and scattered radiation. In particular, the Drane modification of the known Bohren–Huffman algorithm⁶ makes it possible to calculate the parameters Q_{abs} and Q_{pr} with the required accuracy in quite a wide range of the diffraction parameter values (up to $\rho \geq 200$). The FORTRAN programs S1 and S7 from the monograph by Barber and Hill⁷ were also used. They make it possible to calculate the parameters $I(r)$, Q_{abs} , and Q_{pr} up to $\rho = 200$ and $|m| \geq 1.5$. The modified Bohren–Huffman algorithm⁶ taking into account the results from Ref. 8 and realized in the software package Mathematica 3.0 was used for calculating the factor J_1 .

Characteristic types of atmospheric aerosol and their optical constants

Absorption properties of homogeneous particles of atmospheric aerosol consisting of mainly one chemical compound and the so-called model particles, the properties of which will be described below, are analyzed in this paper. A lot of papers are known which are devoted to the determination of optical constants of water and ice and their dependence on temperature in a wide range of the radiation spectrum (see, for example, Ref. 9). So the calculated results for pure water droplets, moderate salted seawater, and spherical particles of amorphous ice are presented below. Silicates, the best studied of which is the amorphous quartz, are the widespread chemical components of particles. It is known⁹ that the values n and κ of chalcedony are most suitable for calculation of the optical characteristics of

SiO₂ present in aerosols. The presence of iron and aluminum oxides significantly affects the complex refractive index of the atmospheric aerosol substance.⁹

In particular, we have analyzed the absorption properties of the hematite (Fe₂O₃) and corundum (Al₂O₃) particles. Sulfur is one of a few chemical elements, which can exist in a free state. Sulfates are the most important component of finely dispersed fraction of atmospheric aerosols. Water solutions of sulfur acid and ammonium sulfate are typical components of the aerosol of volcanic and anthropogenic origin.¹⁰ For this reason, the properties of sulfur acid (H₂SO₄) and ammonium sulfate ((NH₄)₂SO₄) solution droplets were analyzed. Soot of natural and anthropogenic origin also is an important component of tropospheric and stratospheric aerosols. The role of soot in absorption of solar radiation by the Earth's atmosphere is very important. One can consider the primary soot particles formed in the processes of thermal destruction and burning of carbon-containing particles as spherical. The data on optical constants of the particles selected for the analysis are presented in the Table for two wavelengths $\lambda = 0.5$ (spectral maximum of the intensity of solar radiation in the atmosphere) and $10.6 \mu\text{m}$ (radiation of the gas-discharge CO₂ laser).

Optical constants of particles in the calculations of MOC

Particle substance	$\lambda = 0.5 \mu\text{m}$		$\lambda = 10.6 \mu\text{m}$		Ref.
	n	κ	n	κ	
Pure water	1.334	$1.32 \cdot 10^{-9}$	1.144	0.0671	10
Moderately salted sea water	1.342	$2.4 \cdot 10^{-10}$	1.189	0.082	11
Ice	1.312	$1.0 \cdot 10^{-4}$	1.153	0.124	10
Amorphous quartz (SiO ₂)	1.535	$5 \cdot 10^{-4}$	1.51	0.0496	10
Hematite (Fe ₂ O ₃)	3.025	0.0154	1.70	0.259	10
Corundum (Al ₂ O ₃)	1.78	$5.0 \cdot 10^{-4}$	0.58	$5.0 \cdot 10^{-4}$	11
50% solution of sulfur acid (H ₂ SO ₄)	–	–	1.535	0.192	11
Ammonium sulfate ((NH ₄) ₂ SO ₄)	1.52	$5.0 \cdot 10^{-4}$	1.98	$2.0 \cdot 10^{-3}$	10
Soot	1.82	0.74	2.42	1.02	10

Obviously, the aforementioned selection of particles for subsequent analysis of their optical characteristics is quite arbitrary and always is limited. Therefore, in the frameworks of the problem on modeling the optical characteristics of atmospheric aerosols (direct problem of optics of the aerodisperse systems) it is necessary to formulate the problem on modeling the optical constants of the particulate matter. This problem is urgent for the development of optical models of the atmosphere and is considered in Refs. 9, 10, and 12. The technique based on recommendations and conclusions of Ref. 9 was used in calculations. The values n and κ were set for the so-called model particles from a possible range, which does not violate the Kramers–Kronig relationships. The model particles within wide ranges $n = 1.0$ – 3.0 and $\kappa = 10^{-5}$ – 5.0 were considered in the paper. Obviously, that range of the optical constants makes it possible to simulate the absorption properties of all principal types of atmospheric aerosol.

Discussion of the results

1. Intensity of the internal field

Two ways for presentation of the density of electromagnetic wave in the particle volume are known from literature. The first one is calculation of the local source function $B(\mathbf{r})$ (see, for example, Refs. 8, 13, and 14), and the second one is calculation of the mean over the angle⁷ intensity of the internal field $I(r)$. The source function $B(\mathbf{r})$ for unpolarized monochromatic radiation taking into account axial symmetry of the problem can be presented in the form¹³:

$$B(r, \theta, \varphi) = \frac{1}{2\pi} \int_0^{2\pi} \frac{|E(r, \theta, \varphi)|^2}{E_0^2} d\varphi = B\left(r, \theta, \frac{\pi}{4}\right), \quad (1)$$

where $E(r, \theta, \varphi)$ is the local intensity of the electric field inside the particle, E_0 is the amplitude of the incident wave, θ and φ are the polar and azimuth angles in the spherical coordinate system with the origin in the center of the particle. The mean intensity of the internal field over the angles $I(r)$ can be written as follows⁷:

$$\begin{aligned} I(r) &= \frac{1}{4\pi} \int_0^{2\pi} \int_0^{\pi} (EE^*) \sin \theta d\theta d\varphi = \\ &= \frac{E_0^2}{2} \int_0^{\pi} B(r, \theta, \varphi) \sin \theta d\theta. \end{aligned} \quad (2)$$

Both ways provide a descriptive idea on the distribution of electromagnetic energy inside the particle. Authors of this paper used the presentation described in Ref. 7.

As seen from Fig. 1, one can select three characteristic groups of particles depending on the values $m(\lambda)$ at a fixed wavelength: weakly, moderately, and strongly absorbing the radiation. The results obtained for the amorphous quartz particle at $\lambda = 0.5 \mu\text{m}$ and $\rho = 100$ are shown in Fig. 1a. It is characteristic the prevalence of absorption at the rear side of a particle along its main diameter (the result of the focusing effect of the sphere). The intensity of internal field at $\rho = 100$ can exceed the intensity of incident radiation by more than 140 times. One can see analogous dependences for pure water and moderately salted seawater droplets, ice particles, and particles of ammonium sulfate. All these regularities allow one to relate them to the group of weakly absorbing particles. However, the prevalence of absorption, in the front area, that is characteristic of strongly absorbing particles, is observed for the same particles at $\lambda = 10.6 \mu\text{m}$ and quite large ρ (Fig. 1b). Obviously, dividing the particles into the characteristic groups depending on their absorption properties should take into account not only chemical composition of aerosols, but also the characteristics of incident radiation.

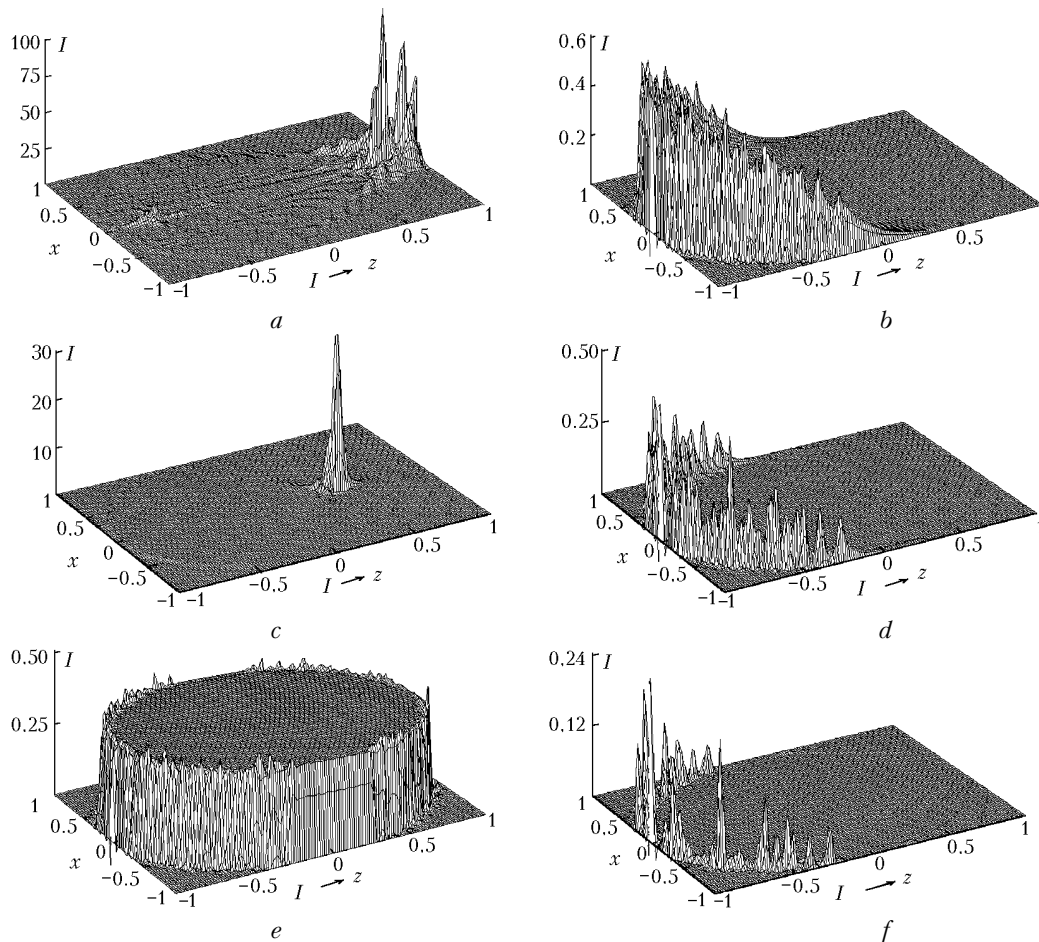


Fig. 1. Intensity of the internal field $I(r)$ for different groups of atmospheric aerosols: amorphous quartz particle, $\lambda = 0.5 \mu\text{m}$, $\rho = 100$ (a); the same, $\lambda = 10.6 \mu\text{m}$, $\rho = 100$ (b); hematite particle, $\lambda = 0.5 \mu\text{m}$, $\rho = 100$ (c); the same, $\lambda = 10.6 \mu\text{m}$, $\rho = 100$ (d); soot particle, $\lambda = 0.5 \mu\text{m}$, $\rho = 100$ (e); the same, $\lambda = 10.6 \mu\text{m}$, $\rho = 100$ (f).

The corundum particles demonstrate interesting peculiarities of the internal absorption. They are typical representatives of weakly absorbing particles at $\lambda = 0.5 \mu\text{m}$ ($m = 1.78 + 5 \cdot 10^{-4}i$) at big ρ . The maxima of distribution of internal intensity at $\lambda = 10.6 \mu\text{m}$ ($m = 0.58 + 5 \cdot 10^{-4}i$) are situated not on the main diameter of the particle (as at $\lambda = 0.5 \mu\text{m}$), but in the ring zone of the front area of the particle. This fact is in complete agreement with the results obtained in Ref. 5.

Moderately absorbing particles (for example, hematite) show the following peculiarities of the internal field. They focus very effectively the radiation in the limited area in the middle of the rear side of the particle at big ρ , and the intensity of internal field can exceed the intensity of incident radiation by tens of times.

Soot particles are typical representatives of strongly absorbing aerosols. Intense absorption in a thin surface front layer (Fig. 1f) is characteristic of them. However, it is peculiar to only large soot particles, but the Rayleigh particles show practically homogeneous absorption over the volume, that is characteristic of the particles of any groups of absorption at small ρ (Fig. 1e). These results make an evidence of only relative correctness of widely used optothermodynamical model of particles absolutely absorbing the radiation in a thin surface layer.

2. Radiation absorption efficiency factor

The radiation absorption efficiency factor Q_{abs} is quite well studied characteristic of not only optically homogeneous^{2,3,16} but also multi-layer spherical particles.^{4,5} So, only most general calculated results of this important characteristic are presented below. The dependence of Q_{abs} on ρ for ice at $\lambda = 0.5 \mu\text{m}$ (weakly absorbing particles) is shown in Fig. 2a. It is seen that the value Q_{abs} increases as ρ increases, the resonance structure of different periodicity is present (morphologically caused resonances²), the absolute values Q_{abs} are relatively small. The particles of quartz, corundum, ammonium sulfate, and seawater droplets have similar dependences. Sharp increase of Q_{abs} and then certain threshold value at $\lambda = 10.6 \mu\text{m}$ are observed for ice particles as ρ increases. The dependence of Q_{abs} on ρ for soot has different view. The resonance structure is practically absent, absolute values of Q_{abs} are quite large. Such a situation is characteristic of soot at both $\lambda = 0.5$ (Fig. 2e) and $\lambda = 10.6 \mu\text{m}$ (Fig. 2f).

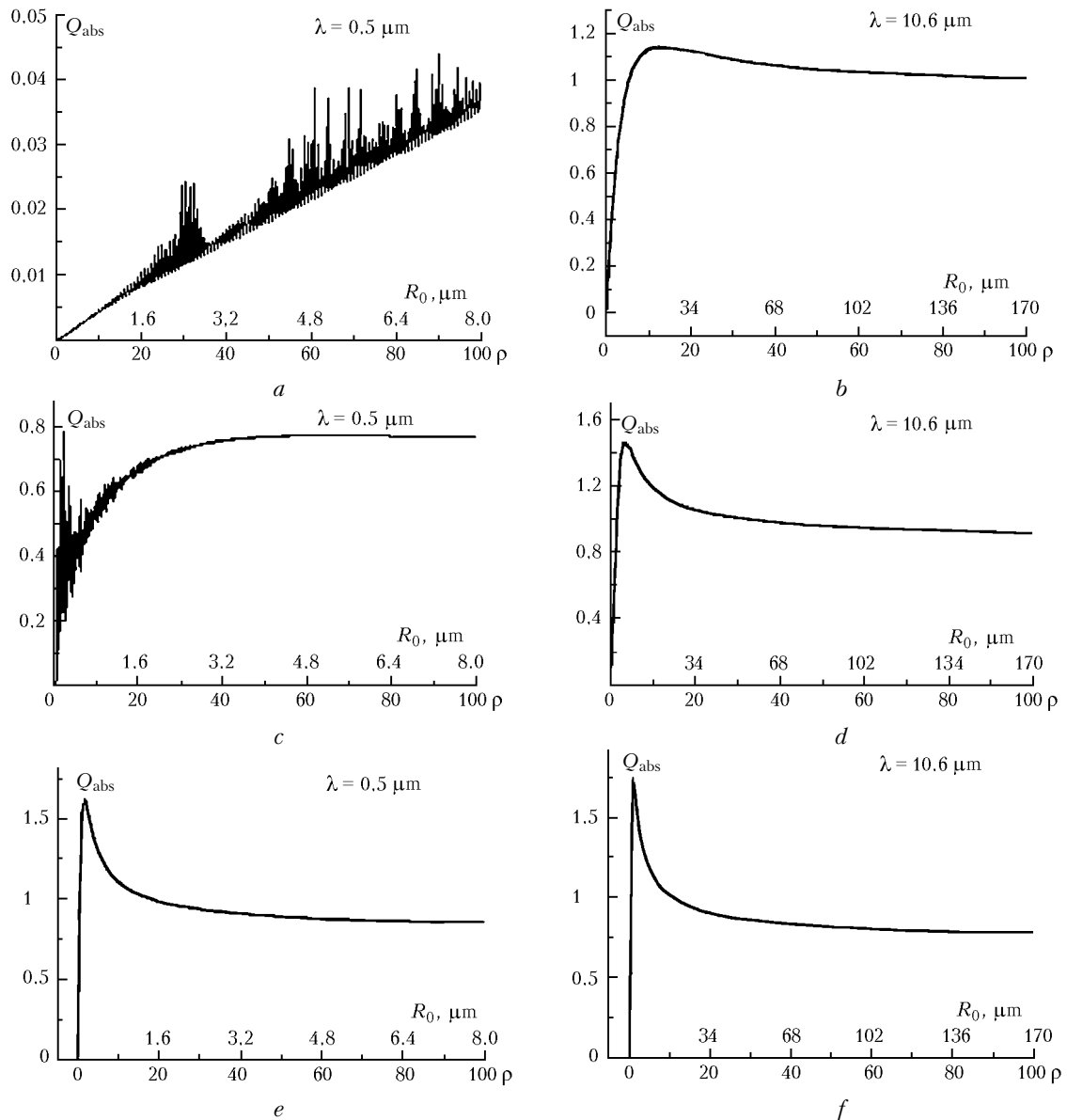


Fig. 2. Radiation absorption efficiency factor Q_{abs} as function of ρ for different groups of atmospheric aerosol: ice particle, $\lambda = 0.5 \mu\text{m}$ (*a*); the same, $\lambda = 10.6 \mu\text{m}$ (*b*); hematite particle, $\lambda = 0.5 \mu\text{m}$ (*c*); the same, $\lambda = 10.6 \mu\text{m}$ (*d*); soot particle, $\lambda = 0.5 \mu\text{m}$ (*e*); the same, $\lambda = 10.6 \mu\text{m}$ (*f*).

3. Light pressure efficiency factor

Exchange of momentum between electromagnetic field and particle occurs at interaction of radiation with aerosol, that causes the light pressure force F_{pr} :

$$F_{\text{pr}} = \pi R_0^2 |E_0^2| Q_{\text{pr}} / (8\pi). \quad (3)$$

According to Ref. 17, the process of the momentum exchange can be divided in two stages: “capture” of field energy by a particle and its partial “reradiating” causing return of the momentum to the field. Thus, the light pressure factor Q_{pr} is naturally involved into the complex of the studied MOC, though it is not directly related to thermal effect of absorbed radiation. It is necessary to consider it when comparing the values of photophoretic and light pressure forces,

and the axis, but not the radial, light pressure force will be of the primary interest below.¹⁸

The dependences of Q_{pr} on ρ for the corundum particles are shown in Figs. 3*a* and *b*. Sharp increase of Q_{pr} as ρ increases is firstly observed at $\lambda = 0.5 \mu\text{m}$, then sharp maximum occurs, and the threshold value is observed at big ρ , which depends on the optical constants of the particle. Such behavior is characteristic of all weakly absorbing particles at $\lambda = 0.5 \mu\text{m}$. Monotonic increase of Q_{pr} as ρ increases is observed for them at $\lambda = 10.6 \mu\text{m}$ (at least, for the values $\rho = 100$), on the background of which the resonances of small amplitude are noticeable. The dependences of Q_{pr} on ρ for hematite (weakly absorbing particles) are shown in Figs. 3*c* and *d*. Sharp increase of the value Q_{pr} is again observed at small values of the diffraction parameter

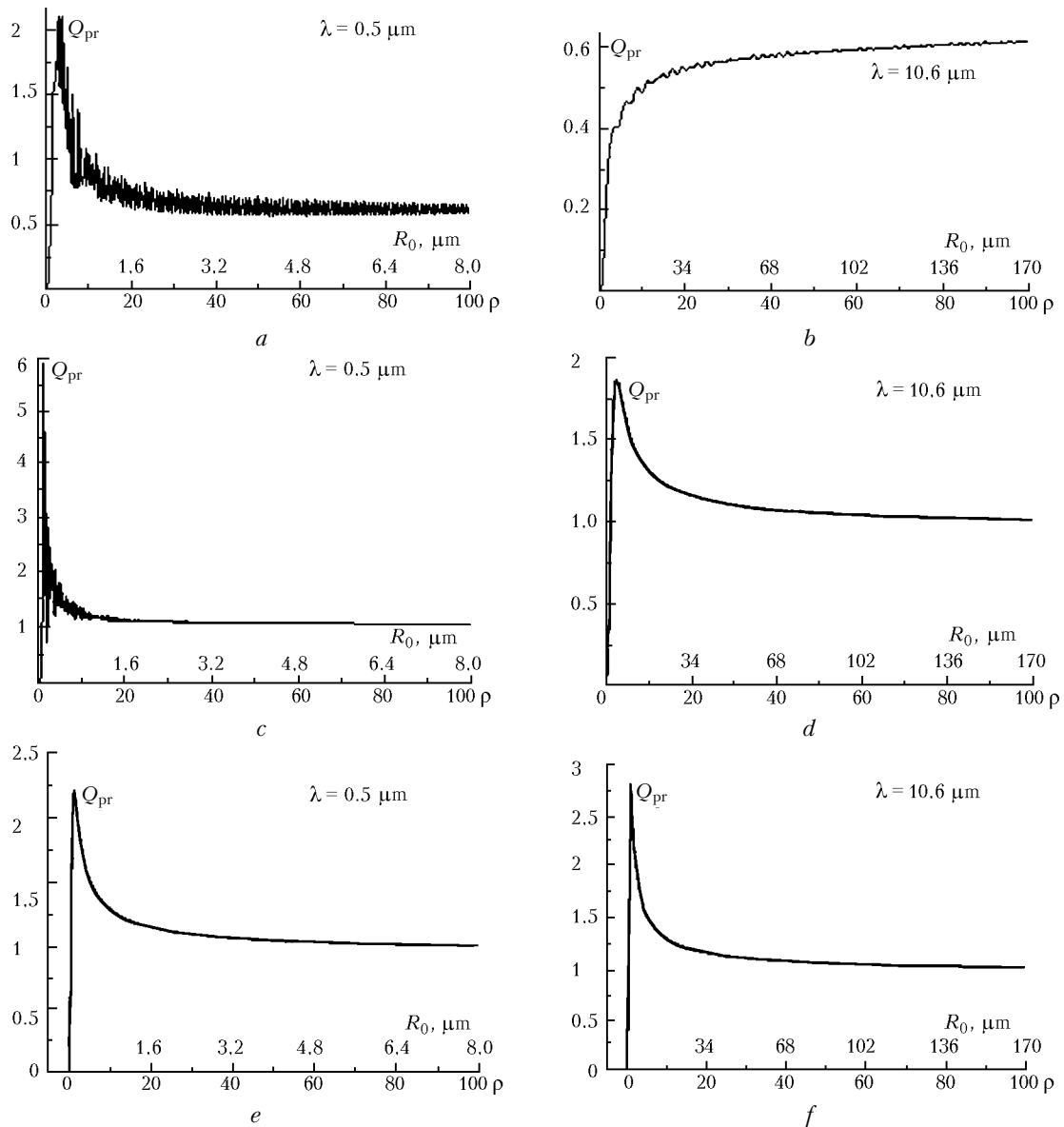


Fig. 3. Light pressure efficiency factor Q_{pr} as a function of ρ for different groups of atmospheric aerosol: corundum particle, $\lambda = 0.5 \mu\text{m}$ (a); the same, $\lambda = 10.6 \mu\text{m}$ (b); hematite particle, $\lambda = 0.5 \mu\text{m}$ (c); the same, $\lambda = 10.6 \mu\text{m}$ (d); soot particle, $\lambda = 0.5 \mu\text{m}$ (e); the same, $\lambda = 10.6 \mu\text{m}$ (f).

(its maximum value at $\lambda = 0.5 \mu\text{m}$ is equal to 6 for $\rho = 2$), then the threshold value of the geometric optics is observed. Similarity of the dependences Q_{pr} on ρ for particles of different substances is known for quite a long time.¹⁹ The presence of maxima in the above-mentioned dependences for some particles can be used for manipulations with microparticles in vacuum.

4. Radiation absorption asymmetry factor

The results of systematic calculations of the J_1 factor is presented for the first time in this paper for the main types of atmospheric aerosol, and the general features of this characteristic as a function of n and κ in quite a wide range of the diffraction parameter are revealed. The relation of J_1 to the values of force and

velocity of photophoretic motion of particles is presented in Ref. 1. In particular, the photophoretic force is

$$F_{ph} = -\frac{2\pi}{3} \left(\frac{\pi M}{8RT} \right)^{1/2} R_0^2 I_0 J_1(\rho, m) F(\text{Kn}, \Lambda, \alpha_E, \alpha_\tau, \alpha_n), \quad (4)$$

where M is the molar mass of gas, T is the temperature, R is the universal gas constant, I_0 is the intensity of incident monochromatic radiation, $F(\text{Kn}, \Lambda, \alpha_E, \alpha_\tau, \alpha_n)$ is the complex function of the Knudsen number Kn , the ratio of heat conductivity of particle and gas Λ , accommodation coefficients of the momentum and gas molecules energy on the particle surface. It was revealed that the direction of the velocity of particle motion (positive or negative photophoresis) is completely determined by the sign of J_1 . It is impossible to change the sign of photophoresis force and of the velocity by

changing the gas-kinetic and accommodation characteristics. As the force and velocity of photophoresis linearly depend on the factor J_1 , its numerical values also determine their absolute values. The value J_1 varies in the limits $-0.5 \leq J_1 \leq 0.5$ (front side of the particle is mainly heated at negative values J_1 , and the rear side is heated at positive values). Figuratively saying, the asymmetry factor is related to the position of the gravity center of the internal sources of heat in the particles.

The dependence of J_1 on ρ for seawater droplets at $\lambda = 0.5 \mu\text{m}$ (the value $\kappa \leq 10^{-4}$ for them) is presented in Fig. 4a. The increase of the value J_1 , as ρ increases, modulated by the presence of resonance structure, and small positive values of J_1 are characteristic of such weakly absorbing particles. These particles can undergo only negative photophoresis (i.e., meet the radiation), and the velocities of expected photophoretic motion are

infinitely small. The shape of the dependence for particles with $\kappa \approx 10^{-1} - 10^{-2}$ (moderately absorbing particles) is quite different: J_1 is positive at small and quite moderate (units) values ρ , then passing to the range of negative values and smooth decrease of J_1 as ρ subsequently increases are observed. Then, at $\lambda = 10.6 \mu\text{m}$ J_1 of quartz particle changes sign at $\rho = 12$, while that of hematite particles changes sign at $\rho = 3$ (Fig. 4d).

Thus, particles of the noted substances of different size should exhibit the change of the photophoretic force in the experiment. The dependences of J_1 on ρ for the strongly absorbing particles with $\kappa > 0.1$ (soot) are shown in Figs. 4e and f. The sign of the factor J_1 is negative, that evidences of the case of positive photophoresis. Absolute values J_1 for quite large soot particles are great, that is an evidence of large possible values of the photophoretic force and velocity.

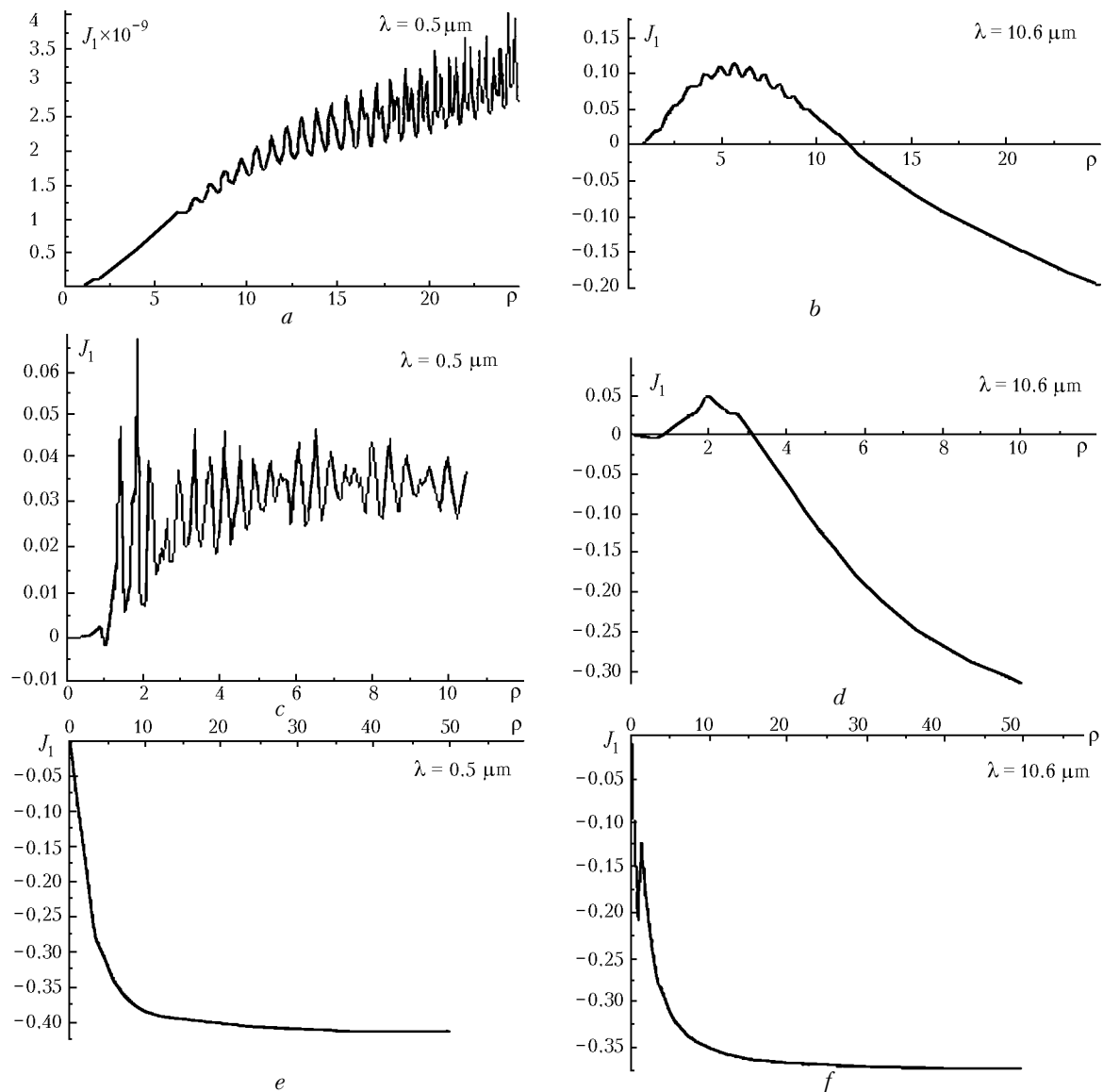


Fig. 4. Radiation absorption asymmetry factor J_1 as a function of ρ for different groups of atmospheric aerosol: seawater droplet, $\lambda = 0.5 \mu\text{m}$ (a); quartz particle, $\lambda = 10.6 \mu\text{m}$ (b); hematite particle, $\lambda = 0.5 \mu\text{m}$ (c); the same, $\lambda = 10.6 \mu\text{m}$ (d); soot particle, $\lambda = 0.5 \mu\text{m}$ (e); the same, $\lambda = 10.6 \mu\text{m}$ (f).

5. Radiation absorption asymmetry factor of model particles

Let us try to generalize the obtained results for J_1 for the so-called model particles. Let us remind, that the values n and κ are set for them, which do not violate the Kramers–Kronig relationships.⁶ The dependences of J_1 on ρ for model particles with $n = 1.0–3.0$ and $\kappa = 0.00001–5.0$ are shown in Fig. 5. The characteristic peculiarity of the particles with $n = 1.5–3.0$ and $\kappa = 0.01–0.1$ is the possibility of both positive and negative photophoresis depending on the particle size at a fixed wavelength of the incident radiation. Absolute values of the positive J_1 are quite large (from 0.03 to 0.15), the range ρ , in which these values are realized, is also quite wide (up to $\rho \approx 10$). Such particles can undergo photophoretic levitation in the upper atmosphere at the relevant gas pressure (gravity force and light pressure force applied to a particle are compensated for by the photophoretic force), or even move upwards in the opposite direction towards solar radiation. This problem is quite traditional (see, for example, Refs. 21–23),

however, no correct models of the vertical transfer of stratospheric and tropospheric aerosols taking into account photophoresis is available to date (recently proposed models^{24,25} have some essential drawbacks).

Conclusion

In this paper, we have presented for the first time the results of systematic analysis of MOC of the main types of atmospheric aerosol. The analysis enabled us to reveal general regularities of the behavior of the characteristics studied. It is planned to continue investigations using the model of two-layer particles, that can approach the expected results to the results obtained for real atmospheric aerosols. It is supposed to use these data for the development of a new model of the vertical transport of stratospheric and tropospheric aerosols, where the photophoretic mechanism will be taken into account in addition to the sedimentation and diffusion mechanisms. Possibly, the calculations made using this model will help us to explain the observed stratification of the stratospheric aerosol.²⁶

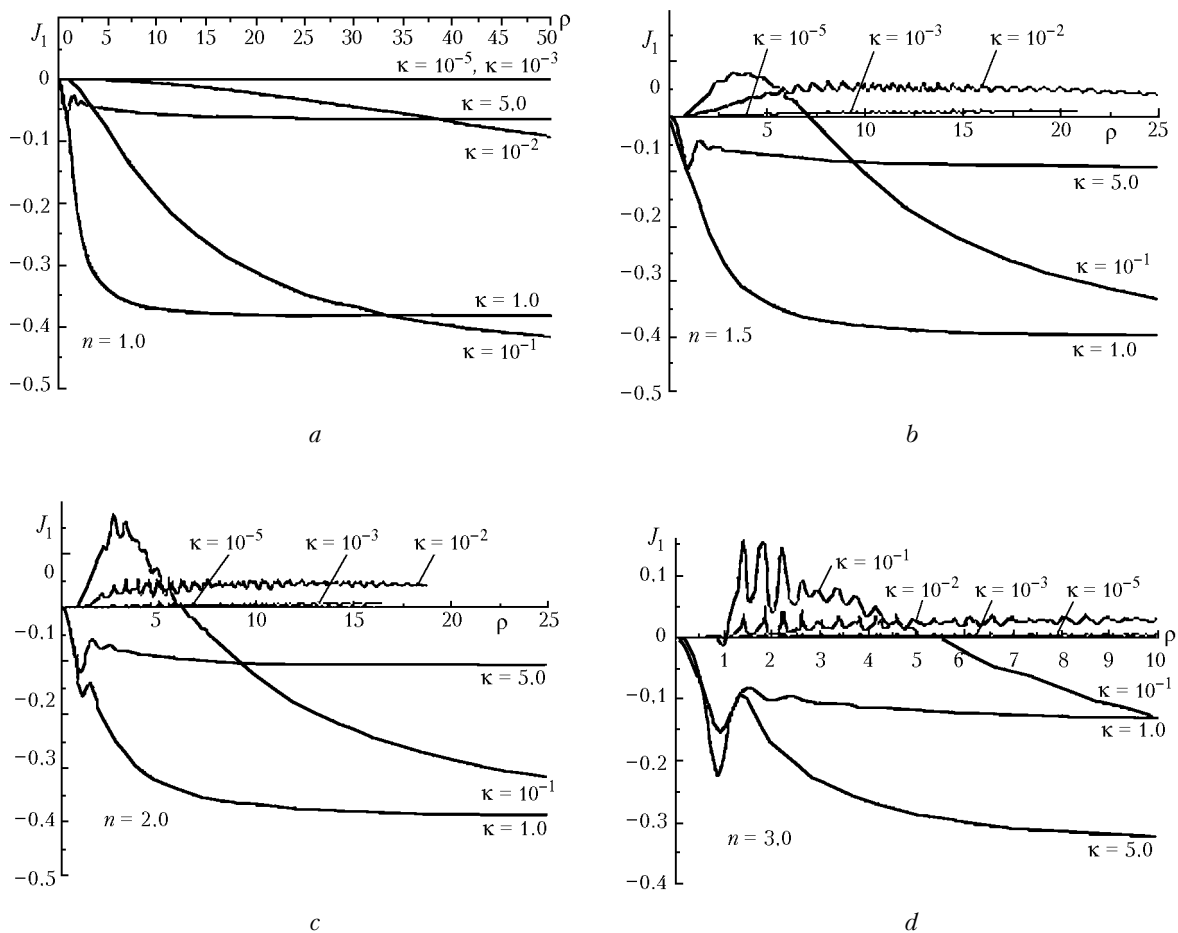


Fig. 5. Radiation absorption asymmetry factor J_1 as a function of the diffraction parameter ρ for model particles with $n = 1.0; 1.5; 2.0; 3.0$ and $\kappa = 10^{-5}; 10^{-3}; 10^{-2}; 10^{-1}; 1.0; 5.0$.

Acknowledgments

The study was supported in part by Russian Foundation for Basic Research (Grant No. 99–01–00143 and No. 01–01–96451) and the Program of Collaboration of the Ministry of Education and Ministry of Defense of Russian Federation “Scientific-Innovation Collaboration”.

References

1. L.B. Letfulova, A.V. Starinov, and S.A. Beresnev, *Atmos. Oceanic Opt.* **14**, No. 1, 69–75 (2001).
2. W.M. Irvine, *J. Opt. Soc. Am.* **55**, No. 1, 16–21 (1965).
3. A.A. Kokhanovsky and E.P. Zege, *J. Aerosol Sci.* **28**, No. 1, 1–21 (1997).
4. A.P. Prishivalko, V.A. Babenko, and V.N. Kuz'min, *Scattering and Absorption of Light by Inhomogeneous and Anisotropic Particles* (Nauka i Tekhnika, Minsk, 1984), 263 pp.
5. D.W. Mackowski, R.A. Altenkirch, and M.P. Menguc, *Appl. Opt.* **29**, No. 10, 1551–1559 (1990).
6. C.F. Bohren and D.R. Huffman, *Absorption and Scattering of Light by Small Particles* (Wiley, New York, 1983).
7. P.W. Barber and S.C. Hill, *Light Scattering by Particles: Computational Methods* (World Scientific Publ., Singapore, 1990), 261 pp.
8. D.W. Mackowski, *Int. J. Heat and Mass Transfer* **32**, No. 5, 843–854 (1989).
9. L.S. Ivlev and S.D. Andreev, *Optical Properties of Atmospheric Aerosols* (State University Publishing House, Leningrad, 1986), 360 pp.
10. V.E. Zuev and G.M. Krekov, *Optical Models of the Atmosphere* (Gidrometeoizdat, Leningrad, 1986), 256 pp.
11. V.M. Zolotarev, V.N. Morozov, and V.E. Smirnova, *Optical Constants of Natural and Technical Media. Handbook* (Khimiya, Leningrad, 1984), 216 pp.
12. K.Ya. Kondratyev, N.I. Moskalenko and D.V. Pozdnyakov, *Atmospheric Aerosol* (Gidrometeoizdat, Leningrad, 1983), 224 pp.
13. P.W. Dusel, M. Kerker, and D.D. Cooke, *J. Opt. Soc. Am.* **69**, No. 1, 55–59 (1979).
14. W.M. Greene, R.E. Spjut, E. Bar-Ziv, A.F. Sarofim, and J.P. Longwell, *J. Opt. Soc. Am. B* **2**, No. 6, 998–1004 (1985).
15. L.G. Astaf'eva and A.P. Prishivalko, *Opt. Spektrosk.* **69**, No. 2, 398–401 (1990).
16. V.E. Zuev, *Propagation of Visible and Infrared Radiation in the Atmosphere* (Halsted Press, New York, 1974).
17. K.S. Shifrin and I.L. Zel'manovich, *Opt. Spektrosk.* **17**, No. 1, 113–118 (1964).
18. V.E. Zuev, Yu.D. Kopytin, and A.V. Kuzikovskii, *Nonlinear Optical Effects in Aerosols* (Nauka, Novosibirsk, 1980), 184 pp.
19. K.S. Shifrin, *Opt. Spektrosk.* **18**, No. 4, 690–697 (1965).
20. A. Ashkin and J.M. Dziedzic, *Appl. Phys. Lett.* **28**, No. 6, 333–335 (1976).
21. C. Orr and E.Y.H. Keng, *J. Atmos. Sci.* **21**, No. 9, 475–478 (1964).
22. R.D. Cadle, *Particles in the Atmosphere and Space* (Reinhold, New York, 1966).
23. S. Tehranian, F. Giovane, J. Blum, Y.-L. Xu, and B.A.S. Gustafson, *Int. J. Heat and Mass Transfer* **44**, 1649–1657 (2001).
24. R. Periasamy, T. Yamamoto, R.P. Donovan, and A.C. Clayton, *J. Electrochem. Soc.* **140**, No. 10, 2949–2951 (1993).
25. R.F. Pueshel, S. Verma, H. Rohatschek, G.V. Ferry, N. Boiadjieva, S.D. Howard, and A.W. Strawa, *J. Geophys. Res. D.* **105**, No. 3, 3727–3736 (2000).
26. A. Cheremisin, L. Granitskii, V. Myasnikov, and N. Vetchinkin, *Proc. SPIE* **4341**, 383–389 (2000).